Pyrolysis kinetics modeling of the hybrid sugarcane IACSP95-5000

Oliveira, T. R., Tannous, K.*

School of Chemical Engineering, University of Campinas
500, Albert Einstein Avenue (Cidade Universitária), Zip code: 13083-852, Campinas/SP, Brazil
*email: katia@feq.unicamp.br; Phone: 55 19 3521-3927; Fax:55 19 3521-3910

Abstract

This work aims to investigate the decomposition reaction kinetics of the hybrid sugarcane IACSP95-5000. The thermogravimetric analyses were conducted using heating rates of 5, 10, 15 and 20 ºC/min in the nitrogen atmosphere. Four thermal decomposition stages were identified: dehydration (25.1–150 °C), extractives (150-240 ºC), pyrolysis (240–420 ºC), and carbonization (420–900 C). The isoconversional methods of Friedman, Ozawa-Flynn-Wall, modified Coats-Redfern and Vyazovkin were applied. The temperature range considered for pyrolysis was 180-420 ºC. The activation energies obtained varied from 159.2 to 163.7 kJ/mol. The best-fit reaction model (Master Plots) was the 6th order reaction. The pre-exponential factor of 1.1 10^{13} s^{-1} considering the activation energy of 152.6 kJ/mol was obtained by the linearization method (average deviation of 22.6%). Besides that, independent parallel reactions scheme for four components (extractives, hemicellulose, cellulose, and lignin) was applied between 150-900 ºC, and the mean activation energies were 131.4, 103.7, 174.1 and 64.0 kJ/mol for four heating rates, respectively, with an average deviation of 4.6%, showing good agreement with the experimental data. Finally, these results can support further energetic availability studies comparative to the others lignocellulosic biomasses.

Keywords: Biomass, sugarcane, kinetics parameters, thermal decomposition, thermogravimetry.

Introduction

One of the world's main concerns in this century is related to the greenhouse effect, global warming and the lack of fossil fuels in the future. As an effort to reduce environmental damages, countries representatives around the world concealed, during the United Nations Conference on Climate Change (COP21) in Paris in December 2015, to create laws in order to maintain the global temperature increase until 2 °C by the end of the 21st century. One of the pillars lies in replacing non-renewable energy sources with natural and renewable ones [1].

Vegetable biomasses configure as a sustainable option to produce heat, electricity, and energy, able to absorb carbon dioxide (main greenhouse gas) during the growing stage and to produce fuels with reduced emission of nitrogenous and sulfurous compounds [2,3]. Even with all these advantages, there is still a fear of using biomass as a source of energy due to two main aspects. Firstly, its use as an energy source competes with food production [4] and secondly, larger technological investments are needed to make biofuels economically competitive compared to fossil fuels [5]. These facts keep conventional oil fuels as the main sources of energy used in agriculture [1], despite their known environmental concerns as non-renewable sources.

Sugarcane is one of the few biomasses in the world able to produce both food and energy. The traditional cane varieties contain high sucrose content for sugar production and the energy canes, with high fiber content, for energy production. This scenario is very important to Brazil, which is the largest producer of sugarcane in the world [6] and encouraged by the Law 6.961/2009. It provides rural credit and technical subsidies for the farmers to produce sugarcane in their properties [7]. All these factors reinforce the need for further studies involving sugarcane as a source of biomass in Brazil.

Sugarcane can be used in different ways for energy production: (1) sugarcane bagasse can produce electricity for the sugarcane plant itself or for other industrial plants [8]; (2) It can also be used to produce second-generation ethanol, charcoal, and bio-oil. Residues such as sugarcane straw or sugarcane bagasse can also be used for thermal processes [9,10].

Different species of sugarcane and residues have already been characterized [7,11,12,13], each one differs in terms of structural aspects, which gives it more or less potential to produce energy. The hybrid varieties, however, created in genetic programs may have a potential for both uses, considering the species used as their parents [8].

The hybrid IACSP-955000 was launched in 2013 by the Agronomic Institute of Campinas composed by the traditional cane Saccharum officinarum and the energy cane Saccharum spontaneum. This specie, which presents higher sugar production, showed better water independence, and higher biomass productivity in drier areas in Brazil. Nevertheless, there are no studies in the literature with this variety to verify if this hybrid can also be used for energy production, maximizing its residues recovery, increasing farmer's profit, and facilitating waste management. The main path to verify energetic potential with this biomass is to investigate the kinetic parameters (e.g., activation energy, pre-exponential factor, and reaction mechanism) of that hybrid and compare it with other energy canes and sugarcane residues reported in the literature.

Then, this study aims to evaluate the thermal decomposition kinetics of the hybrid sugarcane (IACSP95-5000) in the inert atmosphere applying the isoconversional methods (single-step reaction model) and independent-parallel reactions scheme (multiple reactions model). This study may be the first step to maximize the residues recovery of that hybrid (using it for both sugar and energy production) and serve as a guide for design and optimization for pyrolysis with this variety in industrial scale.

Materials and methods

Materials

The biomass used in this work (sugarcane IACSP95-5000) was grown in the Department of Biology of UNICAMP, Brazil, for a period of 18 months. The samples were cut into pieces of 5 cm in length, containing a knot in each piece, and they were cut neglecting the first four knots, due to their higher concentration of phenolic substances [7], which could compromise the kinetic analysis. Due to the high moisture content, the biomass sample was after placed in a drying oven (Quimis, model Q314M-242, Brazil) for 24 hours at 103ºC. After that, the samples were ground and sieved in a RONE knife mill NFA 1533 No. year 44699 coupled with a 6 mm sieve. Granulometric separation was performed in a set of sieves (Produtest, Model T, Brazil) selecting particle diameters between 210-297 µm in order to avoid mass and heat transfer limitation during thermal analysis.

The chemical and thermal properties of the IACSP500 were presented in detail by Lima [14]. In summary the chemical composition (m/m dry basis) was of extractive (67.18%) hemicellulose (13.03%), cellulose (13.70%) and lignin contents (2.82%). The ultimate analysis achieved 42.55 % of carbon, 6.42 % of hydrogen, 0.35 % of nitrogen, and 49.29 % of oxygen (by difference without ash content). The proximate analysis was performed according to standards testing obtaining 78.40 % of volatile matter content, 1.41 % of ash content, and 20.11 % of fixed carbon. The higher heating value, HHV (17.01 ± 0.05 MJ/kg) and the lower heating value, LHV (15.42 MJ/kg) were obtained.

Thermogravimetric Analysis

The thermogravimetric analysis was performed using a thermogravimetric analyzer (Shimadzu Corporation, TGA-50, Japan). The equipment has controlled temperature programming and records the mass variation as a function of time and temperature with measurements uncertainty of 0.001 mg.

The IACSP95-5000 samples were applied in high purity nitrogen (inert) atmosphere (N_2 = 99.996%, 4.6 FID, White Martins, Brazil) with a flow rate of 50 mL/min [7,15]. Four heating rates were used (5, 10, 15 and 20 °C/min) with temperature range (25 ºC - 900 °C). These choices followed the suggestions of ICTAC standards, which proposed to work with 3-5 heating rates lower than 20 ºC/min [16,17]. Higher heating rates interfere with the thermal conversion curves and kinetic parameters, due to limitations in the heat and mass transfer phenomena.

The sample mass applied in the kinetic tests was 10.17 ± 0.23 mg for all heating rates using an alumina crucible with 5 mm of diameter and 4.5 mm of height for all runs. This crucible has a high thermal conductivity, but also chemical stability up to 1750 ºC [17]. The baseline analyses were also performed for the four heating rates to decrease systematic errors and variations in scale measurement due to buoyancy effects with increasing temperature [16].

Data analysis

The baseline and sample data analyses were performed using software Microsoft® Excel 2016 (version 16.0.4266.1001). The mass sample of biomass was firstly subtracted in relation to the baseline, using the PROC function available in the Excel formula package, which searches by the baseline temperature closest to the sample. This procedure was repeated for the entire temperature range for the four heating rates. Baseline data were obtained under the same conditions to the sample in order to eliminate systematic errors as recommended by Vyazovkin *et al.* [17]. The mean difference $(\bar{\xi}_T)$ between the baseline $(T_{baseline_{i,\beta proc}})$ and the sample $(T_{sample_{i,\beta}})$ temperatures were calculated according to Equation 1, in which *T* represent the temperatures data *i* at each time *t*, and *N* represents the numbers of data for each heating rate.

$$\bar{\xi}_T = \frac{1}{N} * \sum_{i=1}^{N} \left| T_{sample_{i,\beta}} - T_{baseline_{i,\beta proc}} \right| \tag{1}$$

The $\bar{\xi}_T$s were lower than 0.7 °C for all heating rates, indicating that both sample and baseline analysis were performed at nearby temperatures, conducting the reliability of the final experimental results for kinetic parameters. A difference greater than 1 °C would implicate in an error of approximately 5% in the estimation of the activation energy and the pre-exponential factor in the pyrolysis region [16].

After this procedure, the DTG (*dm*/*dt*) was calculated in mg/s using Origin 8.1® (version V8.1 SR2) for four heating rates. Thereafter, the noise smoothing of *dm*/*dt* curve was performed as recommended by Vyazovkin *et al.* [16] applying the Fast Fourier Transform Filter for 6 points. According to Vyazovkin *et al.* [17], the noises may be due to an unsatisfactory removal of the products formed in the decomposition of the biomass by the generated gases during the reaction in the TGA. These products are not taken out and accumulate inside the analyzer, which cause noise during the analysis. A noisy analysis of thermogravimetry may affect the application of the isoconversional methods, although it is preferable to use the integral methods in comparison to the differential methods for this type of analysis [16].

After data smoothing, the normalized mass, *W*, and the normalized mass rate, *dW*/*dt*, were calculated according to Equations 2 and 3, respectively, in which m_o and *m* are the mass at the beginning of the analysis and at the temperature *T* and time t, respectively, for each heating rate.

$$W = \frac{m}{m_o} \tag{2}$$

$$\frac{dW}{dt}_{after\ smoothing} = \frac{1}{m_0} * \frac{dm}{dt}_{smoothed} \tag{3}$$

Using the profiles of *W* and *dW*/*dt* as a function of *T* after smoothing, an appropriate temperature range was evaluated to represent the pyrolysis reaction, which satisfactorily represented the entire mass decay. The biomass conversion (α), between 0 and 1, and its conversion rate (*dα*/*dt*) are described by Equation 4 and 5, respectively, in which, W_o, *W*, and W_f represent the normalized masses at the beginning, at time *t* and temperature *T* and at the end of the pyrolysis range, respectively.

$$\alpha = \frac{W_o - W\ (t, T)}{W_o - W_f} \tag{4}$$

$$\frac{d\alpha}{dt} = \frac{1}{(W_0 - W_f)} \frac{dW}{dt}_{after\ smoothing} \tag{5}$$

Kinetic modeling

The biomass decomposition kinetic analysis was performed considering two models: a) single-step and b) multi-step reaction. Considering the first model, the following isoconversional methods were used to estimate the activation energy: the Friedman differential method [18], the Ozawa [19]-Flynn-Wall [20] and the modified Coats-Redfern [21] integral methods, as well as the advanced method of Vyazovkin [22], considering α = 0.05 to 0.95, with a step of 0.05 equidistant from each other. All the methods previously mentioned were applied to the temperature range chosen to represent the pyrolysis reaction.

The Friedman method was performed by the linearization of the natural logarithm of conversion rate, *dα*/*dt* for each conversion in all heating rates as a function of 1/*T* in 1/K (Equation 6). With all the linear functions obtained, the activation energies were calculated by the angular coefficient, considering *R* as the universal gas constant in J/mol.K.

$$ln\left(\frac{d\alpha}{dt}\right)_{\alpha,\beta} = ln\ A + ln\,f(\alpha) - \frac{E_a}{RT_{\alpha,\beta}} \tag{6}$$

The Ozawa-Flynn-Wall method was applied using the linearization of logarithm base 10 of heating rate, β (°C/min), as a function of 1/T in 1/K (Equation 7). The activation energies in all conversions were obtained by the angular coefficient (-0.4567**E*/*R*), where *R* is the universal gas constant in J/mol.K.

$$log\,\beta = log\left(\frac{AE_a}{R\,g(\alpha)}\right) - 2.315 - 0.4567\frac{E_a}{RT} \tag{7}$$

The modified Coats-Redfern method was applied using the natural logarithm of heating rate (β) in °C/min divided by the square temperature, T^2, as a function of 1/T in K (Equation 8). After the linearization in all conversions, the activation energies were obtained by the angular coefficient (-*E*/*R*), in which *R* is the universal gas constant in J/mol.K

$$\ln\left(\frac{\beta}{T^2}\right) = \ln\left(\frac{AR}{E_a g(\alpha)}\right) - E_a/RT \tag{8}$$

The Vyazovkin advanced method is based on the direct numerical integration considering the minimization of the objective function, Ω, described by Equation 9. The solution of this equation was carried out for each conversion level (0.05–0.95) by the minimization function applying optimization tool (SOLVER) with Generalized Reduced Gradient method of MS Excel (version 16.0.4266.1001). Since the integral approximation is given by $I(E\alpha,T\alpha,i)=(E\alpha/R)\,p(x)$, the solution of $p(x)$ was the 8th degree rational approximation, Equation 10, in which $x = E/RT$ [23].

$$\begin{aligned}\Omega = min \sum_{\alpha=0,05}^{0,95} & \frac{I(E_{A,\alpha},T_{\alpha,5})\beta_{10}}{I(E_{A,\alpha},T_{\alpha,10})\beta_{5}} + \frac{I(E_{A,\alpha},T_{\alpha,5})\beta_{15}}{I(E_{A,\alpha},T_{\alpha,15})\beta_{5}} + \frac{I(E_{A,\alpha},T_{\alpha,5})\beta_{20}}{I(E_{A,\alpha},T_{\alpha,20})\beta_{5}} + \frac{I(E_{A,\alpha},T_{\alpha,10})\beta_{5}}{I(E_{A,\alpha},T_{\alpha,5})\beta_{10}} \\ & + \frac{I(E_{A,\alpha},T_{\alpha,10})\beta_{15}}{I(E_{A,\alpha},T_{\alpha,15})\beta_{10}} + \frac{I(E_{A,\alpha},T_{\alpha,10})\beta_{20}}{I(E_{A,\alpha},T_{\alpha,20})\beta_{10}} + \frac{I(E_{A,\alpha},T_{\alpha,15})\beta_{5}}{I(E_{A,\alpha},T_{\alpha,5})\beta_{15}} + \frac{I(E_{A,\alpha},T_{\alpha,15})\beta_{10}}{I(E_{A,\alpha},T_{\alpha,10})\beta_{15}} \\ & + \frac{I(E_{A,\alpha},T_{\alpha,15})\beta_{20}}{I(E_{A,\alpha},T_{\alpha,20})\beta_{15}} + \frac{I(E_{A,\alpha},T_{\alpha,20})\beta_{5}}{I(E_{A,\alpha},T_{\alpha,5})\beta_{20}} + \frac{I(E_{A,\alpha},T_{\alpha,20})\beta_{10}}{I(E_{A,\alpha},T_{\alpha,10})\beta_{20}} + \frac{I(E_{A,\alpha},T_{\alpha,20})\beta_{15}}{I(E_{A,\alpha},T_{\alpha,15})\beta_{20}}\end{aligned} \tag{9}$$

$$p(x) = \left(\frac{exp(-x)}{x}\right) * \left(\frac{x^7 + 70x^6 + 1886x^5 + 24920x^4 + 170136x^3 + 577584x^2 + 844560x + 357120}{x^8 + 72x^7 + 2024x^6 + 28560x^5 + 216720x^4 + 880320x^3 + 1794240x^2 + 1572480x + 403200}\right) \tag{10}$$

Master Plots method

The differential *f*(α) and integral *g*(*α*) conversion functions with the respective phenomena functions were applied based in Mishra *et al.* [25] work (Table 2).

The Master Plots method was used for obtaining the best reaction mechanism represented by the conversion function in its integral form, *g*(*α*), as recommended by the ICTAC [16,24]. The mean activation energy between α = 0.05 and 0.95 obtained by the Vyazovkin Advanced Method (1997) was used for the application of the Master Plots method, due to greater intrinsic accuracy.

The functions of *p*(*x*) and *g*(*α*) were normalized by the α-mean, in which represents the mean point conversion into the range chosen, according to Equations 11 and 12, in which $p(x)_{\alpha,\beta}$ represents the experimental master plots calculated for each conversion point in the four heating rates, $p(x)_{\alpha=0,5}$ refers to the mean conversion point, $g(\alpha)_{\alpha}$ represents the theoretical master plots as a function of conversion applied for each conversion point and $g(\alpha)_{\alpha=0,5}$ is related to the mean conversion point.

$$p(x)_{norm} = \frac{p(x)_{\alpha,\beta}}{p(x)_{\alpha,0,5}} \tag{11}$$

$$g(\alpha)_{norm} = \frac{g(\alpha)_{\alpha}}{g(\alpha)_{\alpha,0,5}} \tag{12}$$

The best reaction mechanism as well as the final temperature range to represent the pyrolysis were chosen by the analysis of the mean relative error of the Master Plots models (ERM_{mp}). Then, it was chosen the scenario which represented the smallest ERM_{mp}, where N is the number of conversions (N=18 points, one for each conversion). The ERM_{mp} was calculated according to Equation 13:

$$ERM_{mp}(\%) = \frac{100}{N}\sum_{i=1}^{N}\left|\frac{p(x)_{norm_{\beta_i}} - g(\alpha)_{norm}}{(p(x)_{norm_{\beta_i}}}\right| \tag{13}$$

Table 2 Differential, *f*(*α*), and integral, *g*(*α*), conversion functions with the respective phenomena. adapted from Mishra et al. [25].

Model	**Formula**	**Differential form *f*(*α*)**	**Integral form *g*(*α*)**
Model 1: Nucleation			
Power-law	P_2	$(2/3)\alpha^{-1/2}$	$\alpha^{3/2}$
Power-law	P_3	$2\alpha^{1/2}$	$\alpha^{1/2}$
Power-law	P_4	$3\alpha^{2/3}$	$\alpha^{1/3}$
Model 2: Sigmoidal Rates			
Avrami-Erofeev	A_1	$(3/2)(1-\alpha)[-\ln(1-\alpha)]^{1/3}$	$[-\ln(1-\alpha)]^{2/3}$
Avrami-Erofeev	A_2	$2(1-\alpha)[-ln(1-\alpha)]^{1/2}$	$[-ln(1-\alpha)]^{1/2}$
Avrami-Erofeev	A_3	$3(1-\alpha)[-ln(1-\alpha)]^{2/3}$	$[-ln(1-\alpha)]^{1/3}$
Area Contraction	R_2	$2(1-\alpha)^{1/2}$	$1-(1-\alpha)^{1/2}$
Volume Contraction	R_3	$3(1-\alpha)^{2/3}$	$1-(1-\alpha)^{1/3}$
Random Nucleation (2)	R_5	$(1/2)\,(1-\alpha)^3$	$1/(1-\alpha)^2$
Model 3: Chemical Reactions			
First Order	F_1	$(1-\alpha)$	$-ln(1-\alpha)$
nth Order	F_n	$(1-\alpha)^n$	$[(1-\alpha)^{1-n}-1]/(n-1)$
Model 4: Diffusion			
Bidimensional	D_2	$[-ln(1-\alpha)]^{-1}$	$\alpha+(1-\alpha)ln(1-\alpha)$
Tridimensional	D_3	$(3/2)(1-\alpha)^{2/3}\,[1-(1-\alpha)^{1/3}]^{-1}$	$[1-(1-\alpha)^{1/3}]^2$
Tridimensional	D_4	$(3/2)[(1-\alpha)^{-1/3}-1]$	$(1-2\alpha/3)-(1-\alpha)^{2/3}$
Zhuravlev	ZH	$(2/3)(1-\alpha)^{5/3}\,[1-(1-\alpha)^{1/3}]^{-1}$	$[1-(1-\alpha)^{-1/3}]^2$

Linearization method

The pre-exponential factor (*A*) was obtained by Equation 14 using the best differential conversion function *f*(*α*) (Table 2) selected by the Master Plots method, in which *dα*/*dt* is the conversion rate in s^{-1} and *A* is the pre-exponential factor in s^{-1}. The parameter *A* was determined by the linear coefficient (*lnA*) and activation energy (E_a) through the angular coefficient. That one should not diverge more than 10% from the E_a obtained by the isoconversional methods, in order to validate the parameters in this method [12,26].

$$\ln\left[\frac{1}{f(\alpha)}\left(\frac{d\alpha}{dt}\right)\right] = \ln A - E_a/RT \tag{14}$$

Independent parallel reactions scheme, IPRS

Considering a more complex biomass decomposition kinetics, such as multiple reactions model, this study applied the independent-parallel reactions scheme (IPRS) for 150-900 ºC, since that the difference between the highest and lowest activation energy ($E\alpha$) as a function of conversion (α) has diverged more than 30% from isoconversional methods [7,12,27,28]. The biomass decomposition between 25-150 ºC was neglected due to the dehydration stage. The activation energies obtained by the isoconversional methods was used as a first guess (for each conversion range) in order to accelerate the process of convergence [13] and to improve fitting data applying multiple steps model [16].

The IPRS considers that the biomass pyrolysis occurs in multiple steps, decomposing simultaneously and separately the extractives, hemicellulose, cellulose, and lignin. In this case, the conversion rate is represented for each component as shown in Equation 15, in which A_i is the pre-exponential factor for each component in s^{-1} and $(d\alpha/dt)_i$ is the conversion rate for each component decomposed. This method uses reaction mechanism $f(\alpha)$ obtained previously by master plots.

$$\left(\frac{d\alpha_i}{dt}\right) = A_i f(\alpha)\exp\left(-\frac{E_{a_i}}{RT}\right) \tag{15}$$

The total conversion rate is the sum of each component calculated previously, according to Equation 16, in which $d\alpha/dt_{theo}$ represents the theoretical conversion rate, n is the number of reactions analyzed (i = 1, 2, 3,…, n), and $(d\alpha/dt)_i$ (Equation 15) is the individual conversion rate of each components reaction, and F_i is the volatilized fraction for each components reaction, where the subtitles represent: E, extractives; HC, hemicellulose; C, cellulose, and L, lignin. Since each component is decomposed generating gases (condensable and non-condensable) and solid products. For the application of Equation 16, it was previously necessary to assume a reaction model of F_n for all the components

$$\frac{d\alpha}{dt}_{theo} = \sum_{i=1}^{n} F_i\left(\frac{d\alpha_i}{dt}\right) = F_E\left(\frac{d\alpha_E}{dt}\right)F_{HC}\left(\frac{d\alpha_{HC}}{dt}\right) + F_C\left(\frac{d\alpha_C}{dt}\right) + F_L\left(\frac{d\alpha_L}{dt}\right) \tag{16}$$

Validation of the single-step model and independent-parallel reaction scheme (IPRS)

To validate the single-step model, the theoretical conversion rate, $(d\alpha/dt)_{theo}$, was calculated during the pyrolysis using all the kinetic parameters obtained by the linearization method: activation energy, pre-exponential factor, and reaction model (Master Plots). The fourth order Runge-Kutta was used for simulation applying an integration step of 5 s for the temperature range chosen for the application of the isoconversional methods.

For the multi-steps model, it was considered that the pyrolysis decomposition reaction occurred in four steps considering the main components: Extractives, Hemicellulose, Cellulose, and Lignin. The following kinetic parameters were varied simultaneously: activation energy, pre-exponential factor, n^{th} reaction order, and volatilized fraction for each reaction for fitting adjustment between the experimental and theoretical conversion rate [13,28,29]. The later one parameter was determined by application of the fourth order Runge-Kutta method considering the integration step of 5 s for the temperature range of 150-900 ºC.

Theoretical data were fitted to the experimental data with least squares method (RSS) [28], Equation 17, in which $(d\alpha/dt)_{i,exp}$, (Equation 5), and $(d\alpha/dt)_{i,theo}$ (Equation 16) correspond to the experimental and theoretical conversion rates, respectively. The number of data applied for the IPRS method for 5, 10, 15 and 20 ºC/min was 1791, 897, 596 and 448 points, respectively, which is lower than the total experimental data concerning to 25-900 ºC (2103, 1061, 712 and 536 points, respectively), due to the elimination of the dehydration region (25-150 ºC) for the application of the IPRS method.

$$RSS = \sum_{i=0}^{N}\left[\left(\frac{d\alpha}{dt}\right)_{i,exp} - \left(\frac{d\alpha}{dt}\right)_{i,theo}\right]^2 \tag{17}$$

The quality of fit (Equation 18) was determined with the average deviation (AD) [28] in which $(d\alpha/dt)_{e,max}$ is the maximum experimental conversion rate, and N is the data points considered.

$$AD(\%) = \left[\frac{\sqrt{\frac{RSS}{N}}}{\left(\frac{d\alpha}{dt}\right)_{e,max}}\right]100 \tag{1b8}$$

The *AD* was minimized for the IPRS method using the optimization tool (SOLVER) in the Excel package. After a first guess of these kinetic parameters, the attempts were repeated until obtaining *AD* values lower than 5% [13,28,29].

Results and discussion

Figure 1 shows the biomass decomposition through the profiles of the normalized mass (*W*) and the normalized mass rate (*dW/dt*) for all heating rates as a function of temperature. It shows the three main events:

(a) The dehydration stage below 150 ºC with normalized mass decay less than 10% (6.37±1.52%);

(b) In the pyrolysis stage, between 180 - 420 ºC, the decomposition of extractives, hemicellulose, and cellulose is more pronounced with mean mass decay of 61.81 ± 0.86%;

(c) In the carbonization stage, from 420 ºC to 900 ºC, there is the formation of carbonaceous residues and stabilization of the mass decay with an average of 11.55 ± 0.85 %.

These events are slightly similar to the reported elsewhere by Carvalho and Tannous [7] and Guimarães [13].

Fig. 1 Normalized mass, *W* and DTG, *dW/dt* as a function of temperature

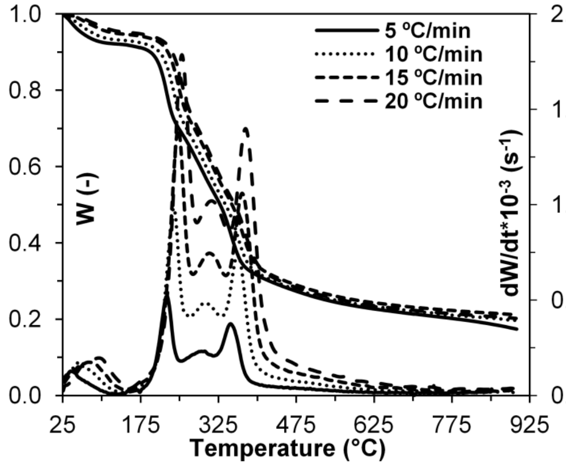

Fig. 2 Apparent activation energies as a function of conversion at 180-420 ºC

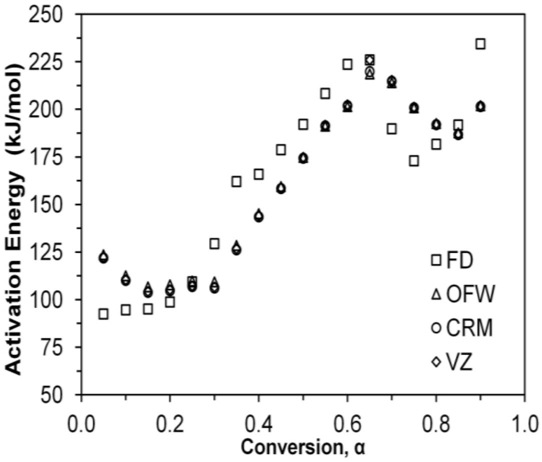

It is also observed (Figure 1) the presence of the three peaks from *dW/dt* related to the decomposition of extractives, hemicellulose, and cellulose, respectively, for the heating rates of 5, 10, 15 and 20 ºC/min:

(a) the first peak, referring to the decomposition of the extractives occurs at the temperatures of 225.8, 236.1, 244.3 and 255.9 ºC (240.5 ± 12.7 ºC);

(b) the second peak refers to the decomposition of hemicellulose at temperatures of 294.2, 297.7, 318.7 and 314.2 ºC (306.2 ± 12.1 ºC), and

(c) the third peak, relative to cellulose decomposition, occurs at temperatures of 352.6, 353.8, 361.1 and 379.4 ºC (361.7 ± 12.4 ºC), respectively.

The lignin decomposition region is not observed in this figure. According to Carvalho and Tannous [7], it is characterized by a low reaction rate and comprehends all the temperature range.

The activation energy profiles as a function of conversion are showed in Figure 2 obtained with all the isoconversional methods applied. The best temperature range for pyrolysis characterization was 180-420 ºC, which satisfactory comprehends the major mass decay region for all the components with nearly 60% of mass decay, The number of data considered to apply the isoconversional methods in that temperature range chosen was 572, 287, 191 and 144 points for 5, 10, 15 and 20 ºC/min, respectively. The integral methods showed similar activation energy profiles in all conversions compared to the differential Friedman method. For the application of the Vyazovkin Advanced Method was the activation energies for each conversion obtained from Friedman. These profiles can represent the four main components in different conversion ranges such as:

(a) for low conversions (0.05-0.02), the activation energies were between 92.5 and 125 kJ/mol, which the extractives govern the decomposition;

(b) after that, there is an increase in the activation energy, reaching peaks closely to 225 kJ/mol between α=0.2 and 0.65, representing the region which hemicellulose governs the decomposition;

(c) at high conversions (α = 0.7 to 0.90), there is a reduction of activation energy profile, indicating the decomposition of cellulose (216.9-.196.0 kJ/mol) This stabilization in high conversions is due to the fact that the biomass was almost decomposed into a carbonaceous residue [12].

The last conversion (α=0.95) varied considerably, especially applying Friedman differential method, reaching higher activation energies (e.g. lignin), due to be very sensitive to noise. Generally, high activation energies are obtained, with variations during conversion [24].

The mean apparent activation energies obtained was of 163.7, 160.3, 159.2 and 159.9 kJ/mol, for FD, OFW, CRM, and VZ methods, respectively, considering the average between them of 160.9 ± 2.4 kJ/mol for 0.05-0.90 of biomass conversion. The last value is slightly lower than the energy canes reported elsewhere, such as Saccharum spontaneum, 164-178 kJ/mol [13], Saccharum robustum, 170-173 kJ/mol [7]. For the residues from sugarcane, bagasse (165-180 kJ/mol) [11] and straw (154-178 kJ/mol) [12], the values were similar in the same range.

The variation between the lowest and highest activation energies (Figure 2) for 0.05-0.90 was 119.3 ± 17.2 % (Figure 2). This variation is much higher than 30% in all the isoconversional methods, thus it is preferable to use multi-steps models [7,12,27,28].

Considering the one-step reaction, only the F_n reaction model was representative for the biomass pyrolysis applying the Master Plots method, as can be seen in Figure 3. The 7th order reaction was the best mechanism (until α=0.60) due to its minor mean relative error ERM_{mp} of 42.59% and at higher conversions: 6th order, at α=0.60-0.70 (ERM_{mp}=12.04%), 5th order at α=0.70-0.80 (ERM_{mp} =14.84%), and 4th order at α=0.80-0.90 (ERM_{mp} =12.16%).

Fig. 3 Master Plots (theoretical) and experimental data considering nth order reaction as a function of conversion

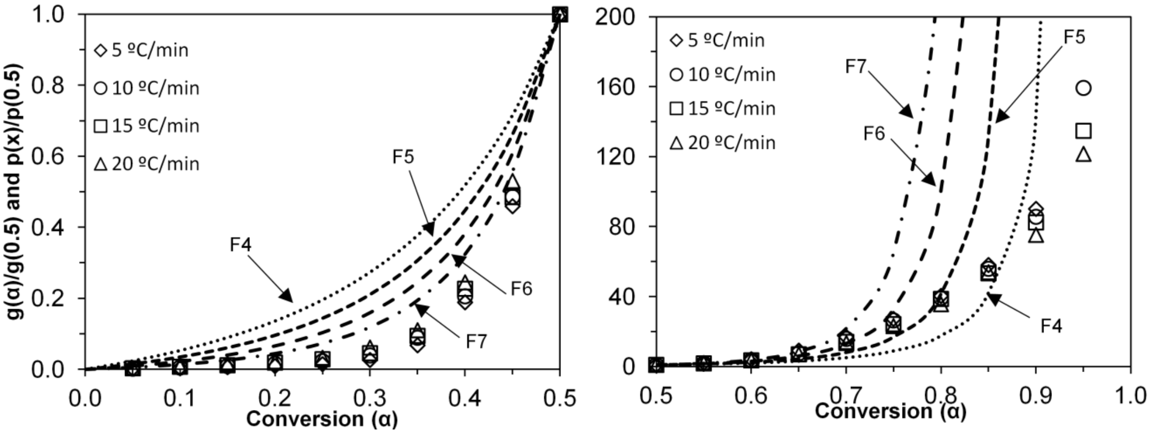

Table 4 and Figure 4 show the results considering the single-step reaction model. Table 4 shows all the parameters obtained by the linearization method (R^2=0.9017). The kinetic parameters were: A=1.1 10^{13} s^{-1} (log A=13.03), E_a=152,6 kJ/mol, and n= F6 at 0.15-0.80 of biomass conversion. In comparison to the activation energy obtained by Vyazovkin method (161.1 kJ/mol), the difference between them was of 5.3%, validating the parameters obtained by that method. In Figure 4, the dotted curve represents the experimental data and the non-continuous curve represents the theoretical data of the conversion rates for all heating rates. The average deviation (*AD*) in this model was 22.6 ± 1.2%. The theoretical data represent the biomass decomposition with one maximum peak varying from 240-260 ºC for 5-20 ºC/min as long as the experimental data comprehends three peaks. This fact suggests not a good agreement with the experimental data for this model.

Table 4 and Figure 5 show the results applying the IPRS considering multi-step reactions for all heating rates. The *AD* was 4.6 ± 1.2%, lower than the single-step model. These results show good agreement with the experimental conversion rates (*AD*<5%) [28,29]. Figure 5 shows the dotted curve which represents the experimental conversion rates from 150-650 ºC for all heating rates (5-20 ºC/min). The results showed that up to 900ºC the conversion rates did not vary significantly. Besides that, it shows four non-continuous curves considering their respective components and decomposition regions: Extractives (180-290 ºC), Hemicellulose (200-370 ºC), Cellulose (260-420 ºC), and Lignin (250-550 ºC).

The temperature ranges of each component decomposition were quite similar to Rueda-Ordónez *et al.* [29] for straw sugarcane, such as hemicellulose (200-400 ºC), cellulose (300-410 ºC), and lignin (300-600 ºC). The global conversion rate curve is represented by the theoretical data obtained by Equation 16.

Table 4: Parameters obtained through the one-step and multiple reaction models.

Heading Rate (ºC/min)	Components	Log *A*	*Ea* (kJ/mol)	n-order reaction	x_i (-)	$AD_{d\alpha/dt}$ (%)
5-20	Single-step reaction	13.03	152.57	6	-	22.64± 1.24
5	Extractives Hemicellulose Cellulose Lignin	11.79 7.24 12.31 1.85	133.73 103.90 174.00 68.24	1 1 1 1.5	0.32 0.21 0.27 0.20	4.61
10	Extractives Hemicellulose Cellulose Lignin	11.25 7.29 12.23 1.91	130.00 103.90 174.00 63.00	1 1 1 1.5	0.33 0.23 0.27 0.17	4.41
15	Extractives Hemicellulose Cellulose Lignin	11.28 7.37 12.22 2.30	131.00 103.90 174.10 63.00	1 1 1 1.5	0.32 0.23 0.27 0.18	4.70
20	Extractives Hemicellulose Cellulose Lignin	11.23 7.33 12.21 2.31	131.00 102.90 174.10 61.90	1 1 1 1.5	0.31 0.24 0.27 0.18	4.72
Mean $AD_{d\alpha/dt}$ (%) (IPRS)						4.61±0.14

Fig. 4 One-step for all heating rates 5º C/min (a) 10 ºC/min (b) 15 ºC/min (c) 20 ºC/min (d), (**o**) experimental (----) theoretical

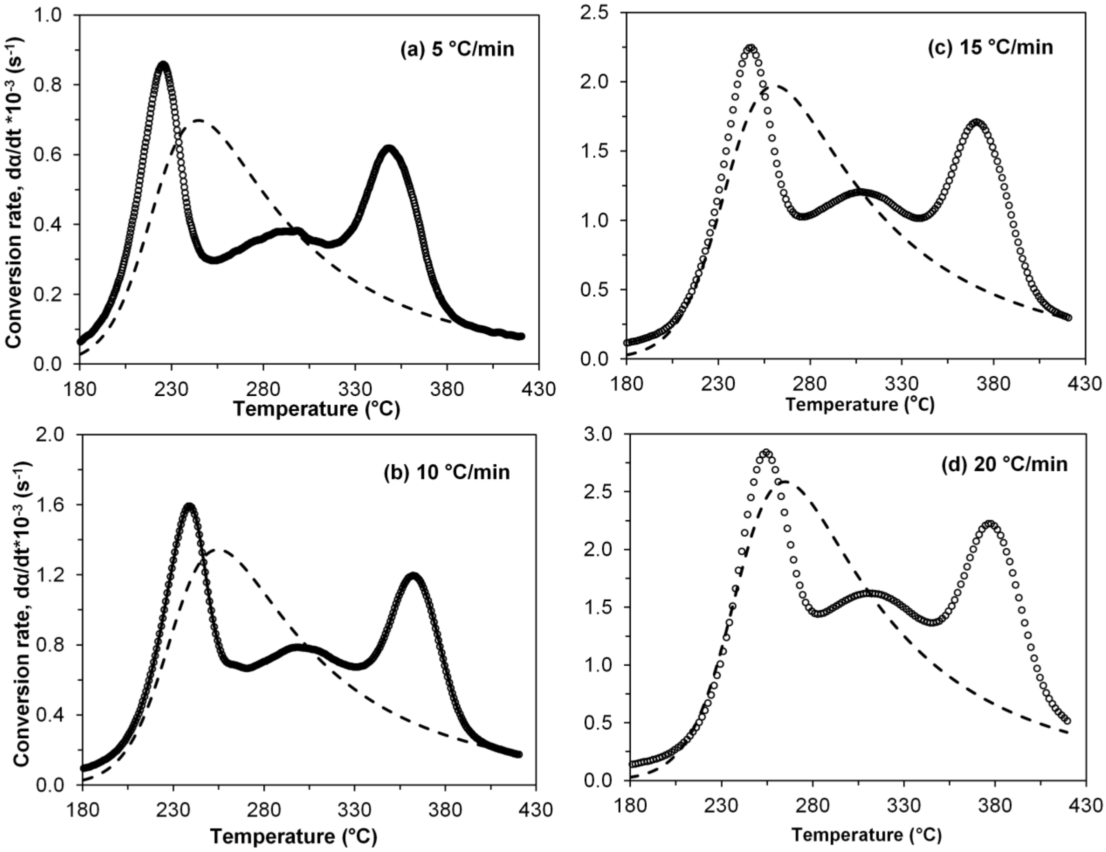

The mean activation energies (Table 4) corresponded to Extractives (131.43 ±1.60 kJ/mol), Hemicellulose (103.65±0.50 kJ/mol), Cellulose (174.05±0.06 kJ/mol), Lignin (64.03±2.85 kJ/mol). These are almost in agreement with the literature for hemicellulose (100-150 kJ/mol), cellulose (180-250 kJ/mol) and lignin (40-100 kJ/mol) [29]. The activation energy for the extractive, however, was higher than the range proposed in the literature (90-110 kJ/mol) [13], but this difference can be justified considering that the extractives content is much more expressive in the hybrid sugarcane compared to other sugarcane residues and energy cane species.

The pre-exponential factors for all heating rates (Log A- Table 4) diverged slightly to Carvalho and Tannous [7], Guimarães [13] and Rueda-Ordóñez *et al.* [29]. This deviation can be justified as reported by Rueda-Ordóñez *et al.* [29], because the pre-exponential factor serves as an adjustment parameter and has no phenomenological meaning.

The nth order reaction for all the components was also in agreement with the literature [12,13], considering order 1 for extractives, hemicellulose, and cellulose. The lignin order most diverged from Carvalho and Tannous [7] and Guimarães [13] considering reaction order of 3 for energy cane, however Rueda-Ordóñez et al. [12] established reaction order of 1 for sugarcane straw. Nevertheless, the reaction order of 1.5 for the lignin led to better fit adjustment than order 3.

The decomposition fraction obtained for each component also promoted better conversion rates fitting for this hybrid, considering the extractives as the main pyrolyzable fraction, which corresponds to the nature of that biomass. This simulation also includes cellulose, hemicellulose and lignin as being the second, third and fourth the greatest fractions, respectively, which agrees with the magnitude of the global and for each conversion rate (Figure 5).

Fig. 5 IPRS results for all heating rates 5º C/min (a) 10 ºC/min (b) 15 ºC/min (c) 20 ºC/min (d)
(o) experimental data; (·····) extractives; (---) hemicellulose, (- - -) cellulose, (-·-) lignin, (—) theoretical

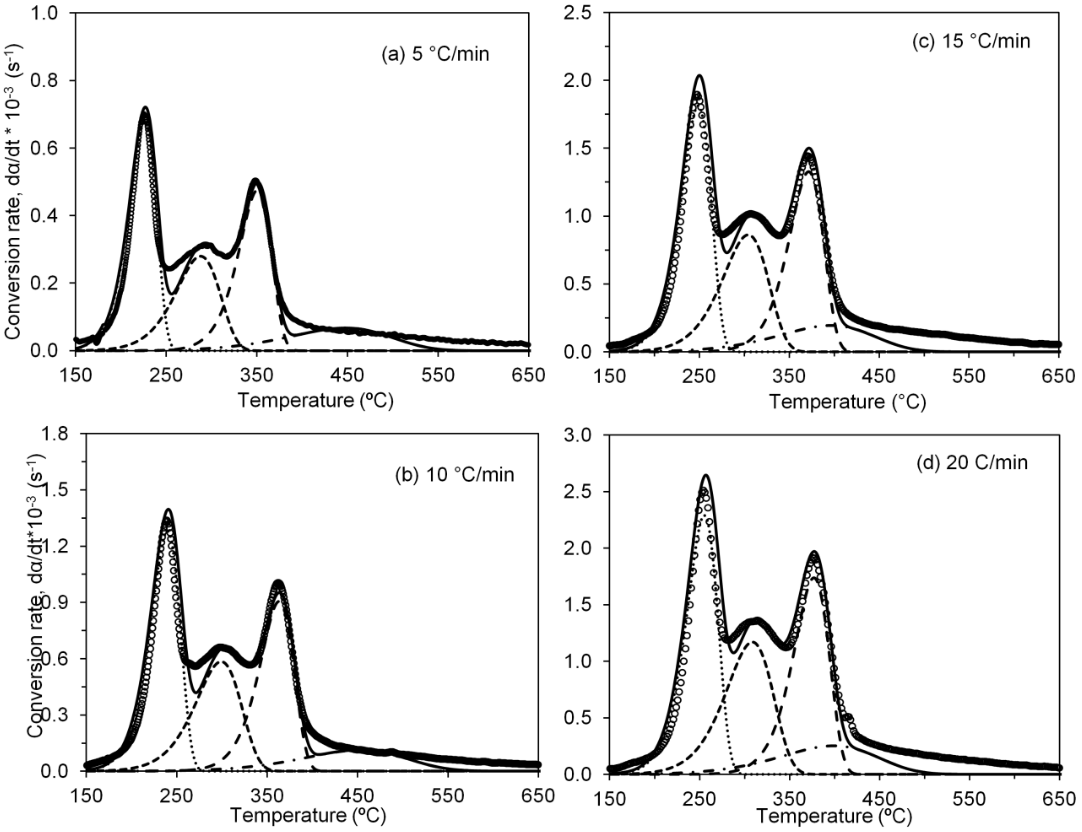

Conclusions

The knowledge of biomass thermal decomposition and kinetic parameters is essential for the design and optimization of the pyrolysis process. The thermogravimetric analysis showed the presence of the main components represented by extractives, pyrolysis, and carbonization. The integral isoconversional methods (Ozawa-Flynn-Wall and Coats-Redfern Modified) as well as Vyazovkin Advanced Method, showed similar behavior in all conversion range concerning the activation energy.

Differently from Friedman, it showed more oscillatory behavior than the others. The one-step reaction model could not be validated due to the high value of the average deviation considering 6th order reaction and temperature range of 180-420 ºC. The kinetic results were better described theoretically applying the IPRS models for four reactions. The activation energies obtained is quite similar for other cane varieties (Saccharum spontaneum and Saccharum robustum) and residues (straw and bagasse sugarcane) considering the hemicellulose, cellulose, and lignin. The activation energy obtained for the extractives diverges slightly from energy canes due to the higher amount of sugar in the hybrid. The reaction orders were in agreement with the literature, although for the residues was closer to the hybrid than the energy cane. The theoretical conversion rates agree with the experimental data and the kinetic parameters obtained could be used to predict different reactions involving pyrolysis. This study can be a support for future studies concerning energy production as well for biofuel production in order to maximize residues recovery and to contribute with sustainability.

Acknowledgements

The authors gratefully acknowledge the financial support from the coordination for the improvement of higher lever Personnel (CAPES) and SAE (UNICAMP), Brazil.

References

1. Gielen, D., Boshell, F., Saygin, D.: Climate and energy challenges for materials science. Nat. Mater. (2016). doi:10.1038/nmat4545
2. Mohan, D., Pittman, C.U., Steele, P.H.: Pyrolysis of wood/biomass for bio-oil: a critical review. Energy Fuel (2006). doi:10.1021/ef0502397
3. Park, Y., Yoo, M.L., Lee, H.W., Park, S.H., Jung, S.C., Park, S.S., Kim, S.C.: Effects Of operation conditions on pyrolysis characteristics of agricultural residues. Renew. Energ. (2012). doi:10.1016/ j.renene.2011.08.050
4. Parajuli, R., Dalgaard, T., Birkved, M.: Can farmers mitigate environmental impacts through combined production of food, fuel and feed? A consequential life cycle assessment of integrated mixed crop-livestock system with a green biorefinery. Sci. Total Environ. (2018). doi:10.1016/j.scitotenv. 2017.11.082
5. Shahbaz, M., Rasool, G., Ahmed, K., Mahalik, M.K.: Considering the effect of biomass energy consumption on economic growth: Fresh evidence from BRICS region. Renew. Sust. Energ. Rev. (2016). doi:10.1016/j.rser.2016.03.037
6. Bonassa, G., Schneider, L.T., Canever, V.B., Cremonez, P.A., Frigo, E.P., Dieter, J., Teleken, J.G.: Scenarios and prospects of solid biofuel use in Brazil. Renew. Sust. Energ. Rev. (2017). doi:10.1016/j.rser.2017.08.075
7. Carvalho, V.S., Tannous, K.: Thermal decomposition kinetics modeling of energy cane Saccharum robustum. Thermochim. Acta, (2017). doi:10.1016/j.tca.2017.09.016
8. Tew, T.L., Cobill, R.M.: Genetic Improvement of Sugarcane (Saccharum spp.) as an Energy Crop. In: Vermerris, W. (eds.) Genetic Improvement of Bioenergy Crops, p. 249-272, Springer, New York (2008).
9. Mesa-Pérez, J.M., Rocha, J.D., Barbosa-Cortez, L.A., Penedo-Medina, M., Luengo, C.A., Cascarosa, E.: Fast oxidative pyrolysis of sugar cane straw in a fluidized bed reactor. Appl. Therm. Eng. (2013). doi:10.1016/j.applthermaleng.2013.03.017
10. Durange, J.A.C., Santos, M.R.L., Pereira, M.M., Fernandes Jr, L.A.P., Souza, M.N., Mendes, A.N., Mesa, L.M., Sánchez, C.G., Sanchez, E.M.S., Pérez, J.M.M., Carvalho, N.M.F.: Physicochemical properties of pyrolysis bio-oil from sugarcane straw and sugarcane in Natura. J. Biomater. Nanobiotechnol. (2013). doi:10.4236/jbnb.2013.42A002
11. Aboyade, A.O., Carrier, M., Meyer E.L., Knoetze, J.H., Görgens, J.F.: Model fitting kinetic analysis and characterisation of the devolatilization of coal blends with corn and sugarcane residues. Thermochim. Acta (2012). doi:10.1016/j.tca.2011.12.007
12. Rueda-Ordóñez, Y.J., Tannous, K.: Isoconversional kinetic study of the thermal decomposition of sugarcane straw for thermal conversion processes. Bioresour. Technol. (2015). doi:10.1016/j.biortech. 2015.07.06215
13. Guimarães, H.R.: Study of the torrefaction of energy cane and its influence over the thermal decomposition kinetics (Master Dissertation), University of Campinas, Brazil. http://repositorio.unicamp.br/jspui/handle/REPOSIP/320801 (2016). Accessed 03 March 2019.
14. Lima, E. C. T.: Energy cane as a potential energy source: characterization of by-products (solid, liquid and gas fractions) from pyrolysis (Master Dissertation), University of Campinas, Brazil. 2016.

http://repositorio.unicamp.br/handle/REPOSIP/321232 (2016). Accessed 05 March 2019. *In Portuguese*.

15. Rueda-Ordóñez, Y.J., Tannous, K.: Drying and thermal decomposition kinetics of sugarcane straw by nonisothermal thermogravimetric analysis. Bioresour. Technol. (2018). doi:10.1016/j.biortech. 2018.04. 064
16. Vyazovkin, S., Burnhamb, A.K., Criado, J.M., Pérez-Maqueda, L.A., Popescu, C., Sbirrazzuoli, N.: ICTAC Kinetics Committee recommendations for performing kinetic computations on thermal analysis data. Thermochim. Acta, (2011).doi:10.1016/j.tca.2011.03.034
17. Vyazovkin, S., Chrissa, K., Laura, M., Lorenzo, D., Koga, N., Pijolat, M., Roduit, B., Sbirrazzuoli, N. Josep, J.: ICTAC Kinetics Committee recommendations for collecting experimental thermal analysis data for kinetic computations. Thermochim. Acta (2014). doi: 10.1016/j.tca.2014.05.036
18. Friedman, H.L.: Kinetics of thermal degradation of char forming plastics from thermogravimetry. Application to a phenolic plastic. J. Polym Sci. A Polym. Symp. 6(*1*), 183-195 (1964)
19. Ozawa, T.A.: A new method of analyzing thermogravimetric data. Bull. Chem. Soc. Jpn. (1965). doi: 10.1246/bcsj.38.1881
20. Flynn, J.H., Wall, L.A.: General treatment of thermogravimetry of polymers. J. Res. Natl. Bur. Stand. 70, 467-523 (1966)
21. Braun, R.L., Burnham, A.K., Reynolds, J.G., Clarkson, J.E.: Pyrolysis kinetics for lacustrine and marine source rocks by programmed micropyrolysis. Energy Fuels (1991). doi:10.1021/ef00025a033
22. Vyazovkin, S.: Advanced isoconversional method. J. Therm. Anal. (1997). doi:10.1007/BF019 83708
23. Pérez-Maqueda, L.A., Criado, J.M.: The accuracy of Senum and Yang’s approximations to the Arrhenius integral. J. Therm. Anal Calorim. (2000). doi:10.1023/A:1010115926340
24. Anca-Couce, A.: Reaction mechanisms and multi-scale modelling of lignocellulosic biomass pyrolysis.: Prog. Energy Combust. Sci. (2016). doi:10.1016/j.pecs.2015.10.002
25. Mishra, G., Kumar, J., Bhaskar, T.: Kinetic studies on the pyrolysis of pinewood. Bioresour. Technol. (2015). doi:10.1016/j.biortech.2015.01.087
26. Jankovic, B.: Kinetic analysis of the nonisothermal decomposition of potassium metabisulfite using the model-fitting and isoconversional (model-free) methods. Chem. Eng. J. (2008). doi:10.1016/j.cej.2007. 07.085
27. Órfão, J.J.M., Antunes, F.J.A., Figueiredo, J.L.: Pyrolysis kinetics of lignocellulosic materials – three independent reactions model. Fuel (1999). doi:10.1016/S0016-2361(98)00156-2
28. Lopes, F.C.R., Pereira, J.C., Tannous, K.: Thermal decomposition kinetics of guarana seed residue through thermogravimetric analysis under inert and oxidizing atmospheres. Bioresour. Technol. (2018). doi:10.1016/j.biortech.2018.09.021
29. Rueda-Ordóñez, Y.J., Tannous, K., Olivares-Gómez, E.: An empirical model to obtain the kinetic parameters of lignocellulosic biomass pyrolysis in an independent parallel reactions scheme. Fuel Process. Technol. (2015). doi:10.1016/j.fuproc.2015.09.001